Supporting information

Highly reversible lithium storage in conversion-type $ZnCo_2O_4$ anode promoted by $NiCl_{2-x}F_x$ hydrate

Jiaojiao Deng,[a‡] Xiaoliang Yu,[b‡] Jie Tang,*[b] Lihan Zhang,[a] Kun Zhang,[b] Shiqi Lin,[b] Baohua Li*[a]

[a] Engineering Laboratory for Functionalized Carbon Materials, Tsinghua Shenzhen International Graduate School, 518055, PR China. E-mail: libh@mail.sz.tsinghua.edu.cn

[b] National Institute for Materials Science, 1-2-1 Sengen, Tsukuba, Ibaraki, 305-0047, Japan. E-mail: tang.jie@nims.go.jp

‡ These authors contributed equally to this work.

Experimental Section

Synthesis of ZCO: $ZnCo_2O_4$ microspheres were prepared according to a solvothermal synthesis method reported in our previous work.[sliced] Typically, 5 mmol of $Zn(NO_3)_2\cdot 6H_2O$, 10 mmol of $Co(NO_3)_2\cdot 6H_2O$ and 180 mmol urea were dispersed in 70 mL of ethylene glycol with continuous stirring. After turning into homogenous solution, the above mixture was transferred into a 100 mL Teflon lined stainless-steel autoclave and heated at 200 °C for 24 hours, before cooling down to room temperature. The obtained products were washed several times by water and ethanol, and collected by vacuum filtration, and then dried in 80 °C oven for 12 hours. Finally, by annealing the precursors at 600 °C for 4 h in air with a heating rate of 1 °C min^{-1}, $ZnCo_2O_4$ microspheres were acquired.

Synthesis of ZCO/H-NCF and ZCO/NCF composites: 1 ml of 4 mM NH_4F aqueous solution was added into 2 ml of 1 mM $NiCl_2$ aqueous solution under vigorous stirring drop by drop. The water was evaporated by heating and stirring the mixture at 85 °C. The resulting sample was annealed at 400 °C for 2 h under Ar atmosphere, with a heating rate of 5 °C min^{-1}, then the $NiCl_{2-x}F_x$ product was obtained. ZCO/H-NCF was prepared by mixing ZCO and $NiCl_{2-x}F_x$ in de-ioned water with a mass ratio of 7:3. The mixture was then heated at 85 °C with stirring until all free water was evaporated. The product was collected and designated as ZCO/H-NCF. ZCO/NCF was further obtained by annealing at 280 °C for 4 h in Ar atmosphere, with a heating rate of 5 °C min^{-1}.

Material Characterization: The morphologies of the materials were checked by field emission scanning electron microscopy (FE-SEM, JSM-6500) and transmission electron microscopy (TEM, FEI Tecnai G2 F30). X-ray diffraction (XRD) patterns were identified on a Rigaku D/max 2500 diffractometer with Cu Kα radiation (λ = 1.5418 Å). An X-ray photoelectron spectroscopy (XPS, PHI 5000 VersaProbe II) was applied to characterize the chemical bonding states of samples and electrode materials upon lithiation/delithiation. Raman spectra of samples were obtained on a Microlaser confocal Raman spectrometer (HORIBA LabRAM HR800). Fourier transform infrared spectroscopy (FT-IR, MDTC-EQ-M13-01) was used to obtain the FT-IR spectra of samples. The thermal stability of the samples was measured by thermogravimetric (TGA, Hitachi HT-Seiko Instrument Exter 6300) in nitrogen heating from room temperature to 400 °C with a heating rate of 10 °C min^{-1}.

Electrochemical Measurement: The lithium storage performance of electrodes was measured by 2032-type coin cells. Active materials (ZCO, ZCO/H-NCF and ZCO/NCF), carbon black (super P) and polyvinylidene fluoride (PVDF) were mixed in N-methyl-2-pyrolidinone (NMP) solvent with a mass ratio of 8:1:1. The obtained slurry was pasted onto copper foil after stirring for 6 h, followed by drying in a vacuum oven for 12 h at 110 °C. Then the electrode film was punched into a disk with a diameter of 15 mm. The mass of the active material was controlled at ≈1 mg cm^{-2}. The electrolyte was $LiPF_6$ (1 M) in a mixed solvent of ethylene carbonate (EC)/diethyl carbonate (DEC) (volume ratio of 1:1). The galvanostatic charge-discharge tests were conducted using a Land 2001A battery test system in a voltage range of 0.01-3.0 V at room temperature. Cyclic voltammetry (CV) tests were performed on a VMP3 electrochemical station with a scan rate of 0.1 mV s^{-1} in the same potential range.

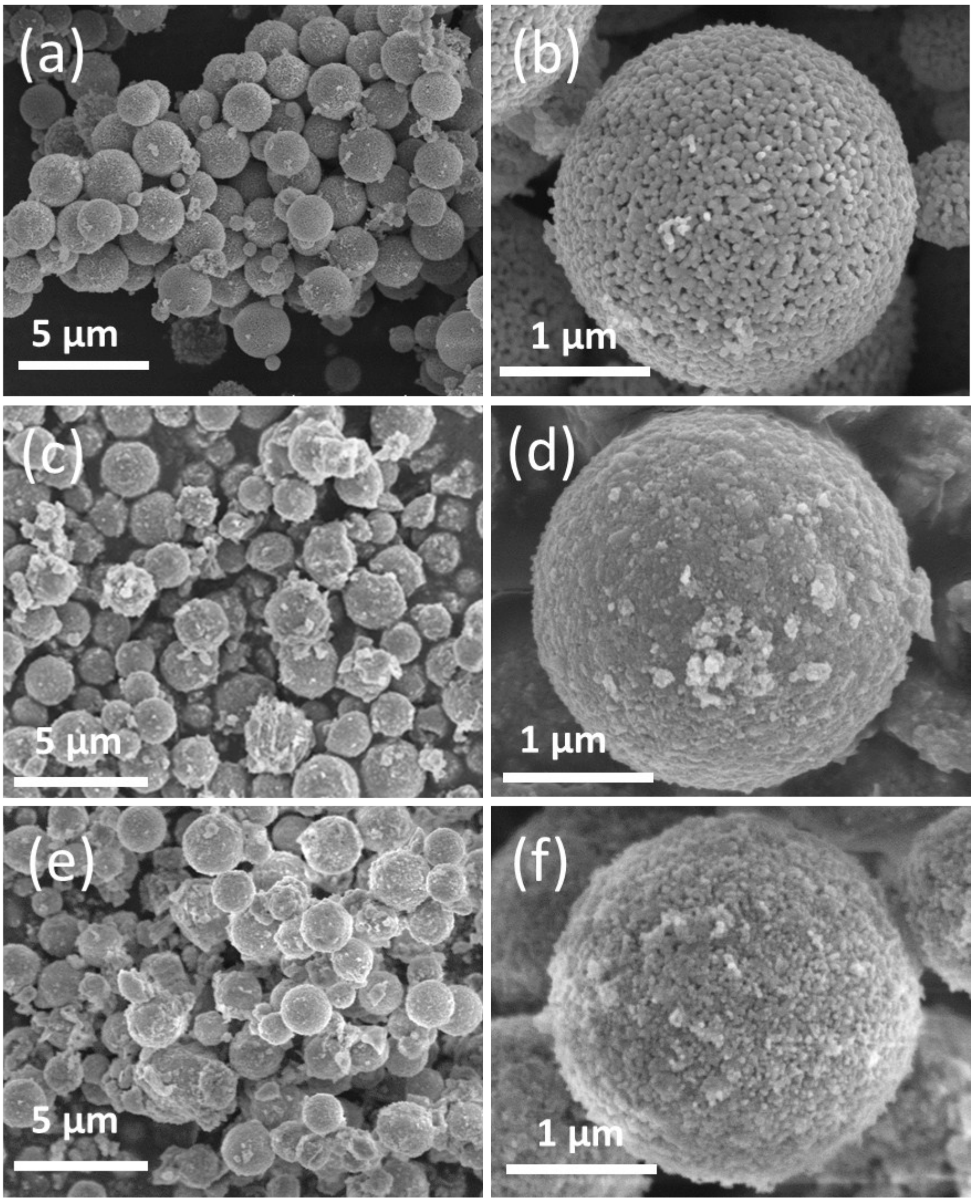

Fig. S1 SEM images of ZCO (a, b), ZCO/H-NCF (c, d) and ZCO/NCF (e, f)

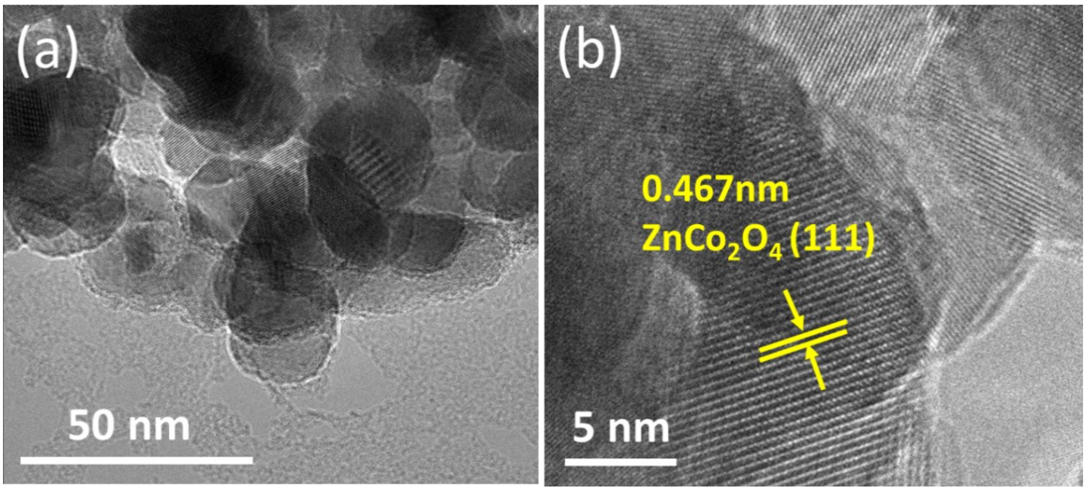

Fig. S2 TEM (a) and HRTEM (b) image of ZCO.

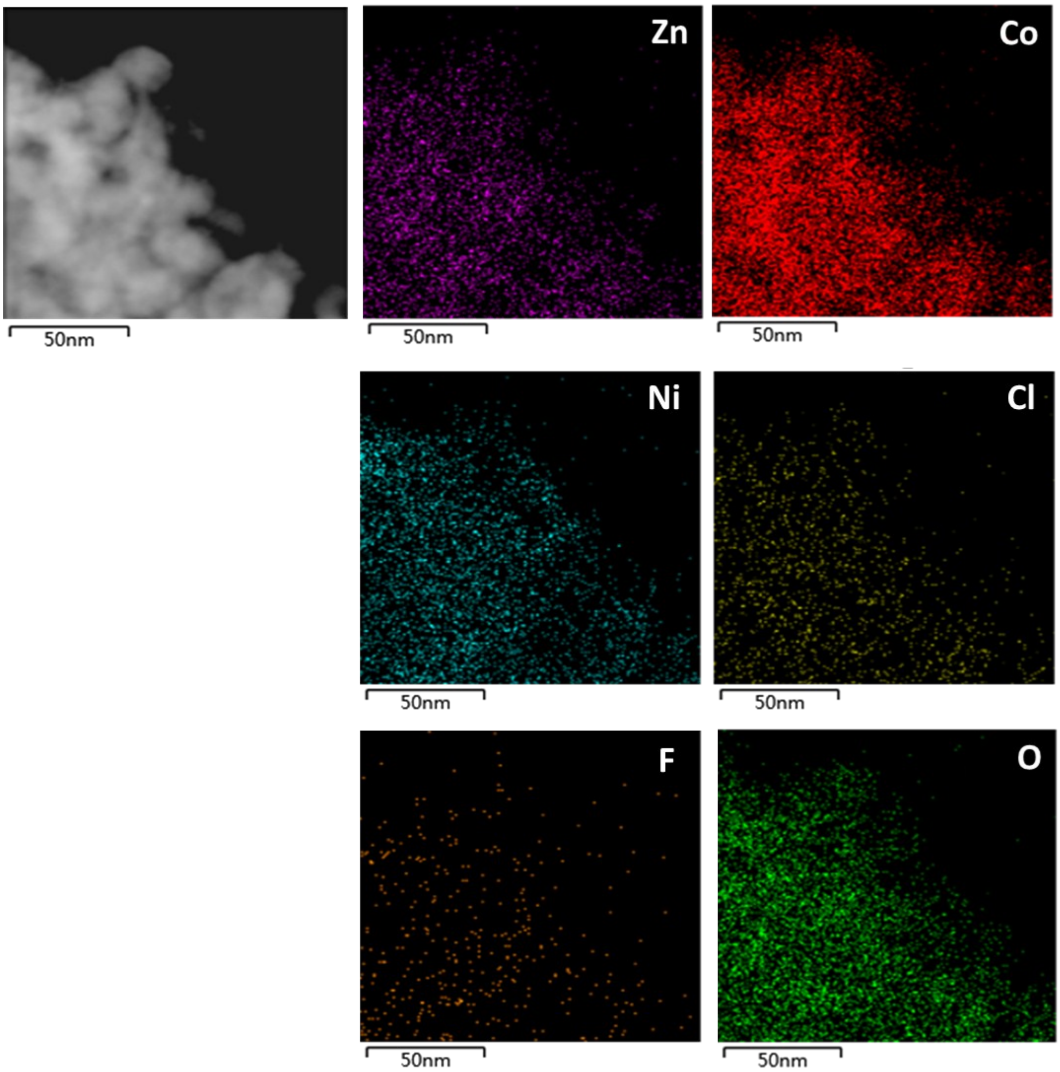

Fig. S3 Dark field scanning transmission electron microscope (STEM) image and corresponding EDS mapping of ZCO/H-NCF.

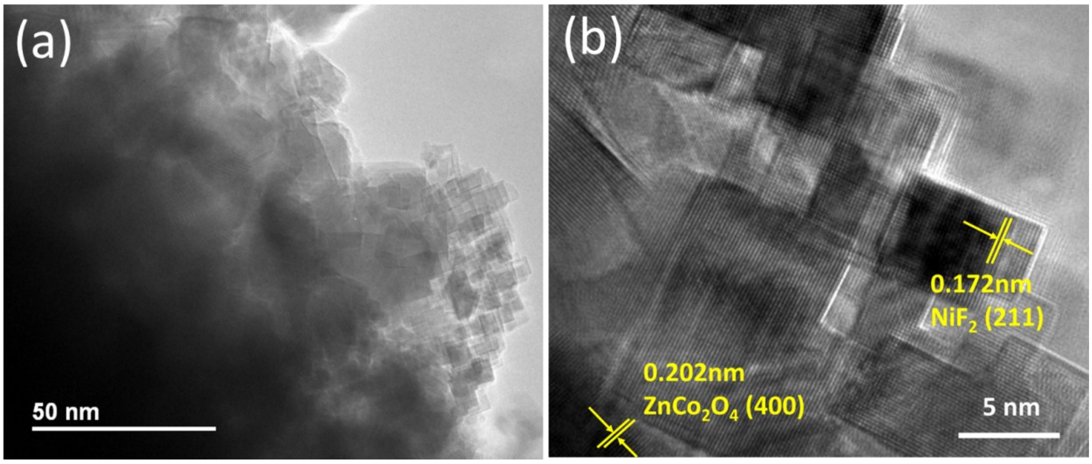

Fig. S4 TEM (a) and HRTEM (b) image of ZCO-NCF.

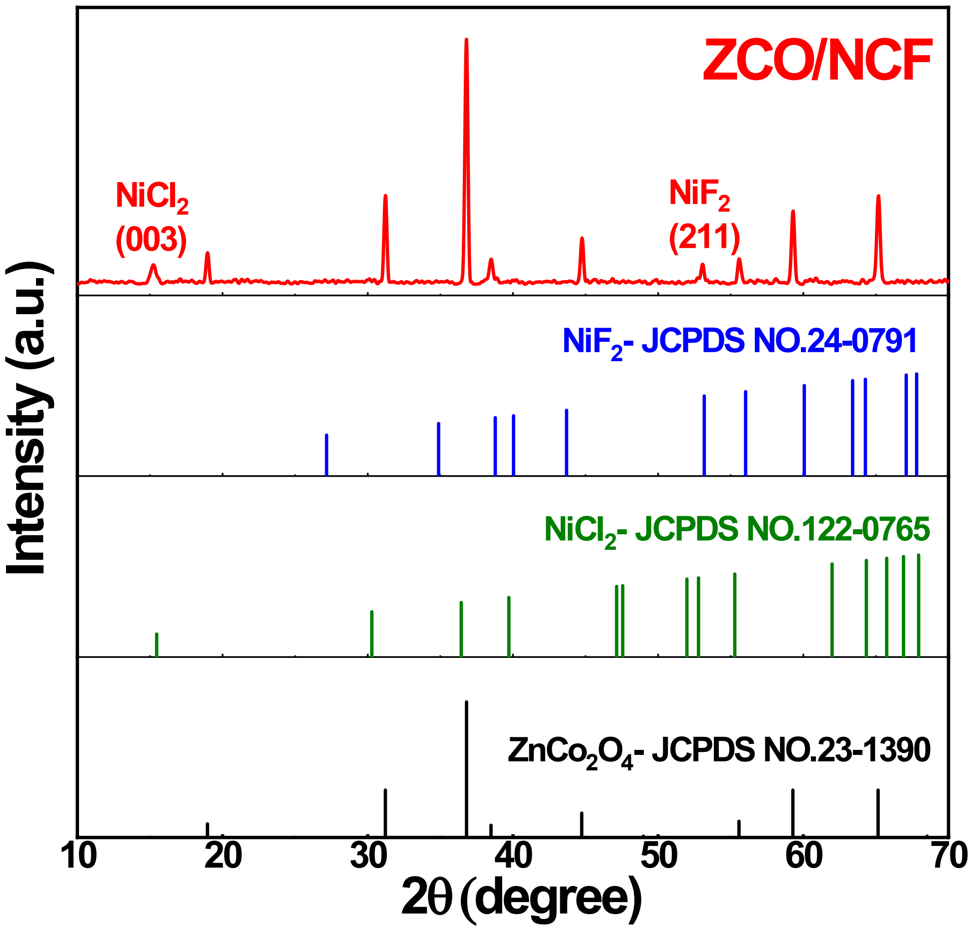

Fig. S5 XRD pattern of ZCO/NCF

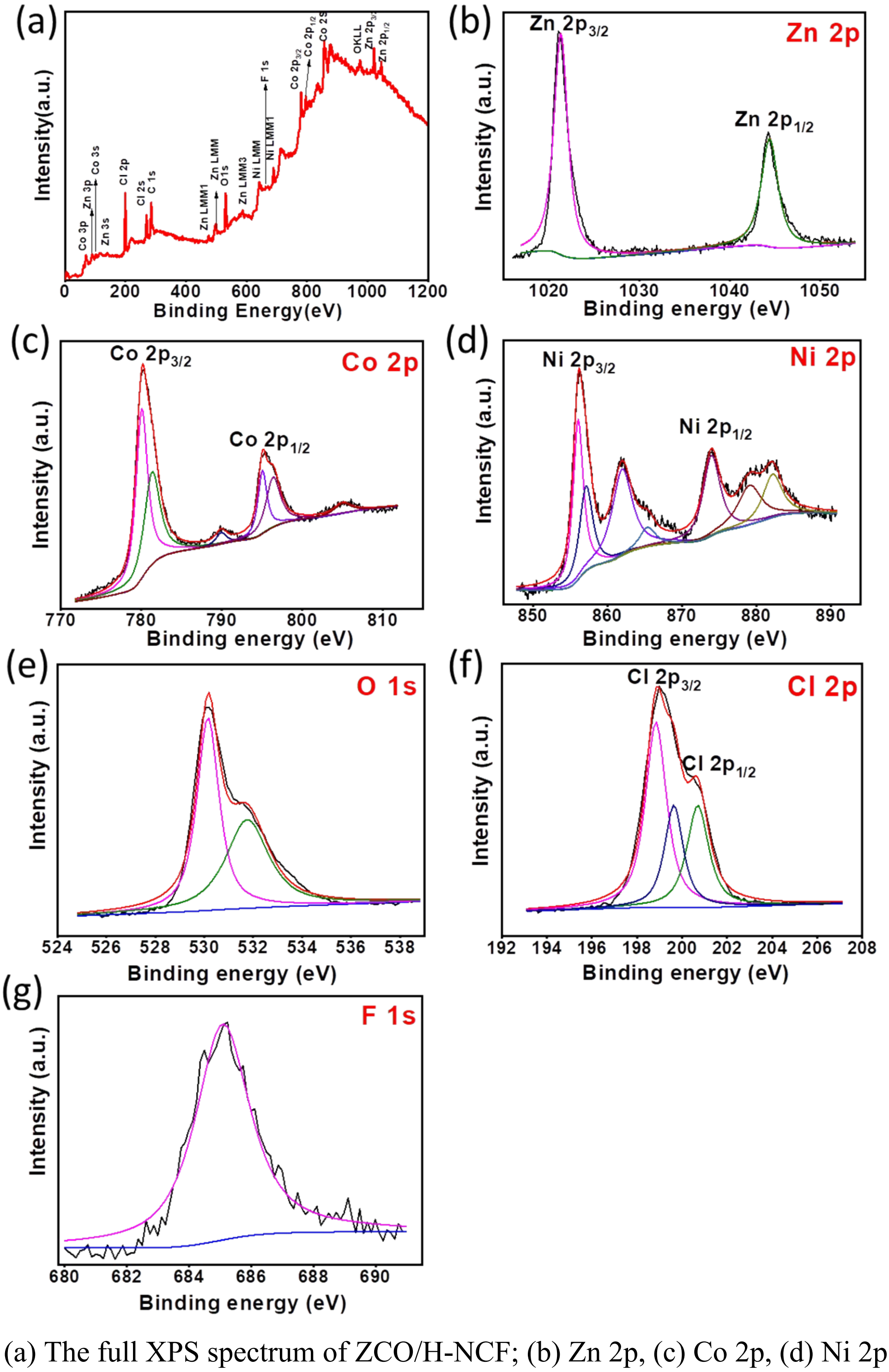

Fig. S6 (a) The full XPS spectrum of ZCO/H-NCF; (b) Zn 2p, (c) Co 2p, (d) Ni 2p, (e) O 1s, (f) Cl 2p, and (g) F 1s XPS spectra of ZCO/H-NCF.

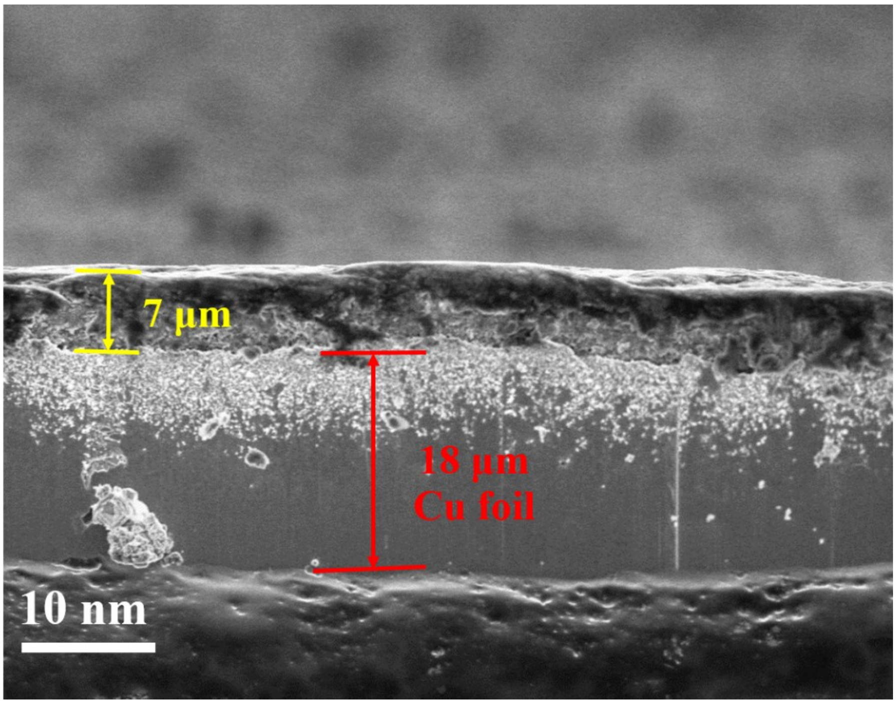

Fig. S7 Cross-sectional SEM image of the ZCO/H-NCF electrode

The areal mass loading is 1 mg cm^{-2} and the thickness is 7 μm, the gravimetric capacity of ZCO/H-NCF electrode was 1089 mAh g^{-1}. Therefore the mass density and the volumetric capacity of the ZCO/H-NCF electrode can be calculated to be 1.43 g cm^{-3} and 1557 mAh cm^{-3}, respectively.

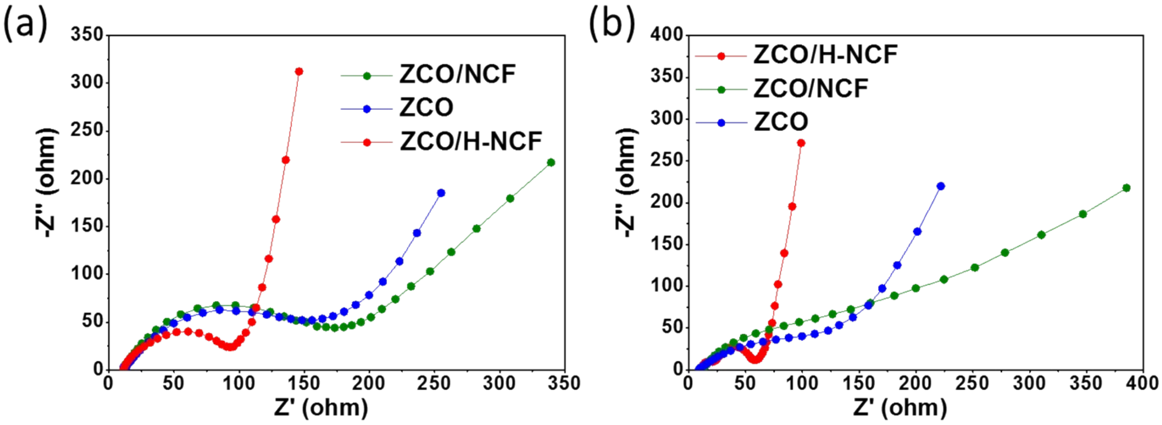

Fig. S8 EIS spectrum of ZCO, ZCO/H-NCF and ZCO/NCF electrodes at pristine state (a) and after 100 cycles at 1 A g^{-1} (b).

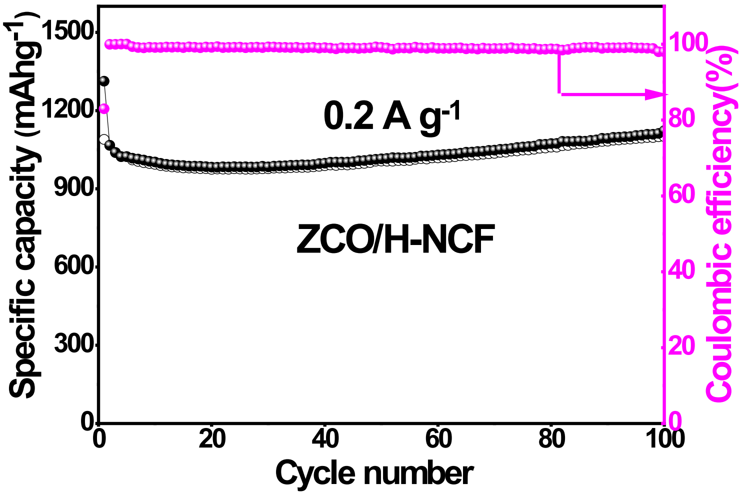

Fig. S9 Cycling performance of ZCO/H-NCF at a current density of 0.2 A g^{-1}.

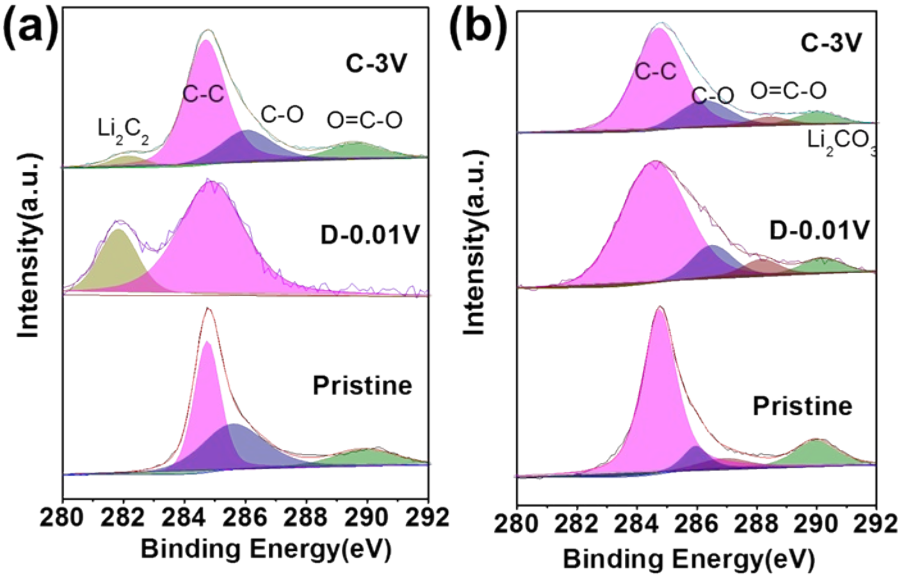

Fig. S10 C 1s XPS evolution of SEI layer in ZCO electrode (a) and ZCO/NCF electrode (b) based on the pristine, fully lithiated, full delithiated states in the first cycle.

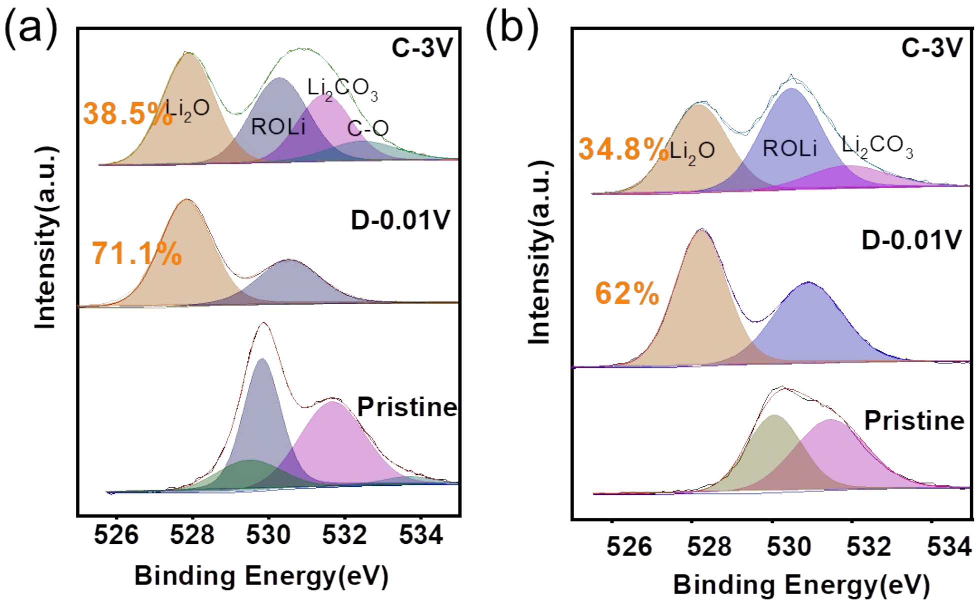

Fig. S11 O 1s XPS evolution of ZCO electrode (a) and ZCO/NCF electrode (b) based on the pristine, fully lithiated, full delitiated states in the first cycle.

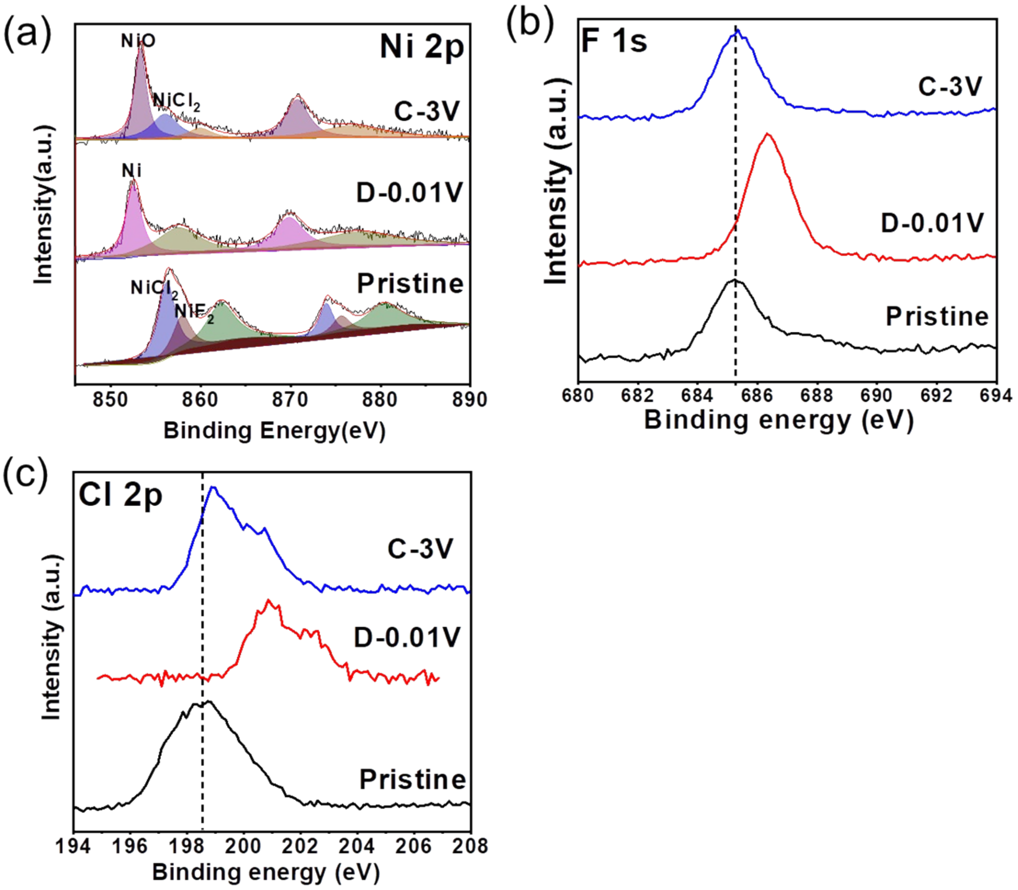

Fig. S12 (a) Ni 2p, (b) F1s and (c) Cl 2p XPS evolution of ZCO/H-NCF electrode based on the pristine, fully lithiated, full delitiated states in the first cycle.

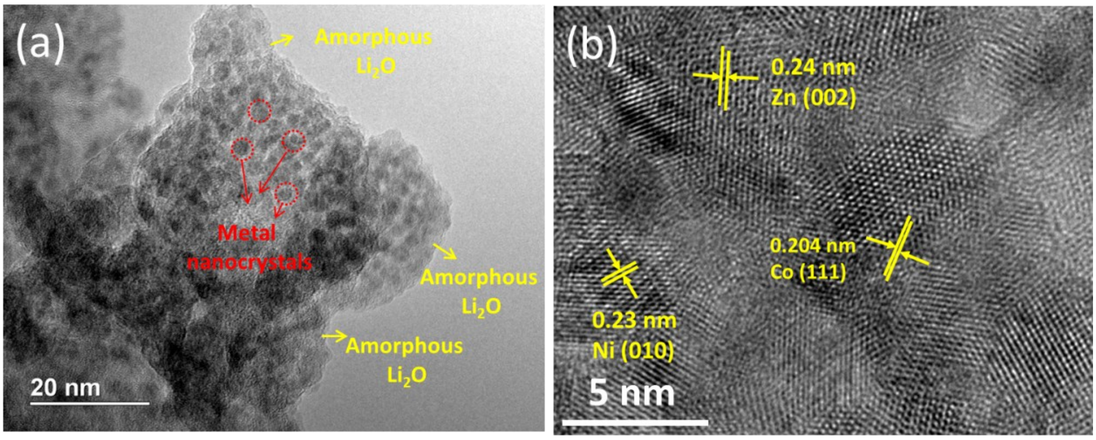

Fig. S13 TEM (a) and high-resolution TEM (b) image of the ZCO/H-NCF electrode after full lithiation.

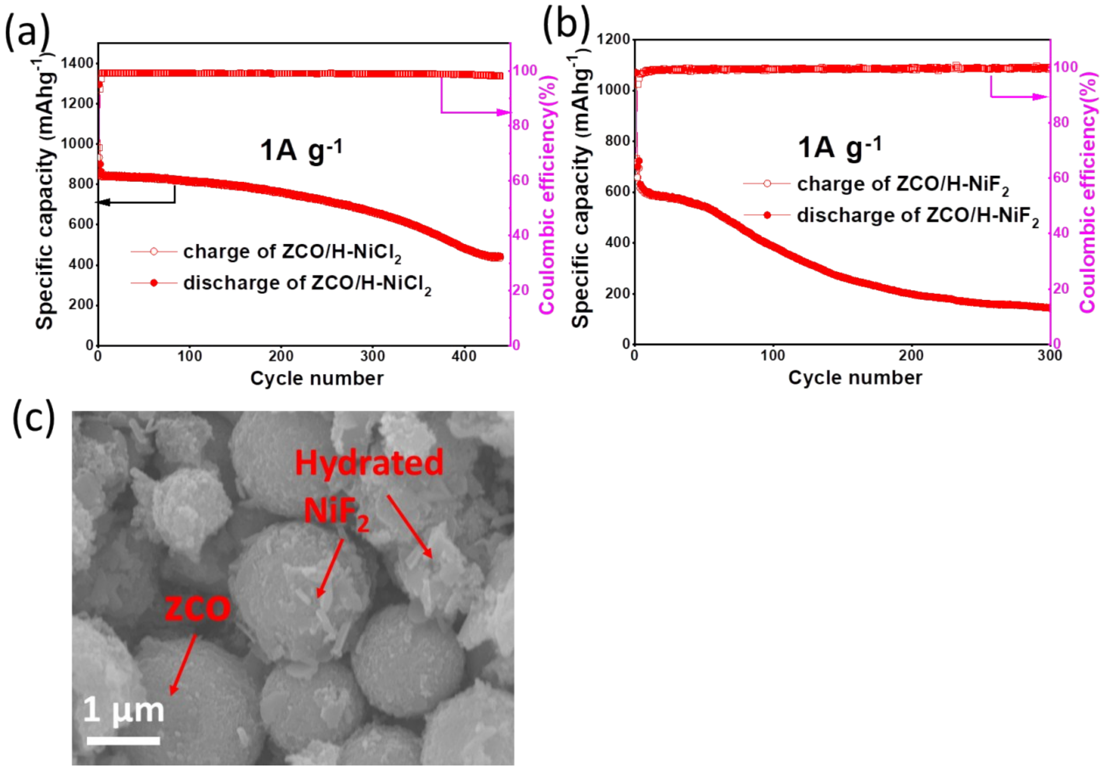

Fig. S14 Cycling performance of the $ZnCo_2O_4$/hydrated $NiCl_2$ hybrid (ZCO/H-$NiCl_2$) (a) and the $ZnCo_2O_4$/hydrated NiF_2 hybrid (ZCO/H-NiF_2) (b) at a current density of 1 A g^{-1}. SEM image of ZCO/H-NiF_2 (c).

ZCO/H-$NiCl_2$ and ZCO/H-NiF_2 were prepared by the same process as that of ZCO/H-NCF except that only $NiCl_2$ or NiF_2 was added during the solution reaction. The electrochemical performance of ZCO/H-NiF_2 is not only poorer than that of ZCO/H-NCF but also much poorer than that of the ZCO anode. This may be ascribed to the low solubility of NiF_2 in water (2.5 g/100 mL). It generates the uneven hybrid of ZCO and H-NiF_2 (see Fig. S14c) during solution synthesis process and thus poor electrochemical performance.

Table S1 Performance comparison between our ZCO/H-NCF anode and previously reported advanced AB_2O_4-type transition metal oxide anodes.

Sample	Initial Coulombic efficiency	Rate performance	Cycling stability	Ref.
$CoFe_2O_4$ Hollow Spheres	72.7% at 0.1 A g^{-1}	46.2% capacity retention at 2 A g^{-1}	70.5% capacity retention over 600 cycles at 1 A g^{-1}	1
$ZnCo_2O_4$ microspheres /$NiSi_x$ nanowires	71.2 % at 0.1 A g^{-1}	26.5% capacity retention at 4 A g^{-1}	72.4% capacity retention over 340 cycles at 1 A g^{-1}	2
$NiCo_2V_2O_8$ Yolk–Double Shell Spheres	60% at 0.2 A g^{-1}	28.6% capacity retention at 10 A g^{-1}	~69% capacity retention over 500 cycles at 1 A g^{-1}	3
Co_3O_4/NiO/C hybrids	60% at 0.2 A g^{-1}	47.4% capacity retention at 4 A g^{-1}	76.5% capacity retention over 1000 cycles at 1 A g^{-1}	4
Hollow Co_3O_4 Microspheres	65.3% at 0.05 A g^{-1}	22.9% capacity retention at 2 A g^{-1}	79.7% capacity retention over 1000 cycles at 1 A g^{-1}	5
ZCO/H-NCF	83% at 0.2 A g^{-1}	66.3% capacity retention at 5 A g^{-1}	75% capacity retention over 1000 cycles at 1 A g^{-1}	This work

References

1. C. Wang, H. Su, Y. Ma, D. Yang, Y. Dong, D. Li, L. Wang, Y. Liu and J. Zhang, *ACS Appl. Mater. Interfaces,* 2018, **10**, 28679-28685.
2. H. Chen, Q. Zhang, J. Wang, Q. Wang, X. Zhou, X. Li, Y. Yang and K. Zhang, *Nano Energy*, 2014, **10**, 245-258.
3. Y. Lu, J. Nai and X. W. Lou, *Angew. Chem. Int. Ed.,* 2018, **57**, 2899-2903.
4. Y. Wang, M. Kong, Z. Liu, C. Lin and Y. Zeng, *J. Mater. Chem. A,* 2017, **5**, 24269-24274.
5. C. Hou, Y. Hou, Y. Fan, Y. Zhai, Y. Wang, Z. Sun, R. Fan, F. Dang and J. Wang, *J. Mater. Chem. A,* 2018, **6**, 6967-6976.